

Electrical Properties of $\alpha\text{Fe}_2\text{O}_3$ and $\alpha\text{Fe}_2\text{O}_3$ Containing Titanium

F. J. MORIN

Bell Telephone Laboratories, Murray Hill, New Jersey

(Received February 9, 1951)

Electrical conductivity, Hall effect, and Seebeck effect have been measured on two sets of polycrystalline samples of $\alpha\text{Fe}_2\text{O}_3$ and $\alpha\text{Fe}_2\text{O}_3$ containing from 0.05 to 1.0 atomic percent titanium (n -type impurity). One set of samples contained 0.6 atomic percent excess of iron (n -type impurity), the second set contained 0.6 atomic percent deficiency of iron (p -type impurity).

The conductivity of pure $\alpha\text{Fe}_2\text{O}_3$ is independent of this amount of stoichiometric deviation. The slope of the log conductivity vs reciprocal temperature plot is 1.17 eV and the intercept at $1/T=0$ is $2.1 \times 10^4 \text{ ohm}^{-1} \text{ cm}^{-1}$. Room temperature conductivity varies from $\sim 10^{-14} \text{ ohm}^{-1} \text{ cm}^{-1}$ (extrapolated) for pure $\alpha\text{Fe}_2\text{O}_3$ to $0.2 \text{ ohm}^{-1} \text{ cm}^{-1}$ for $\alpha\text{Fe}_2\text{O}_3$ containing 1.0 atomic percent titanium.

The measured Hall voltages seem to result entirely from magnetization of the samples, which are weakly ferromagnetic, and disappear above the ferromagnetic Curie temperature.

The temperature variations of the Fermi level are determined from Seebeck data. The temperature variations of carrier concentration are determined from Fermi level and of mobility from carrier concentration and conductivity for some samples. Carrier concentration results indicate that each added titanium ion donates approximately one electron to the conduction process. Mobilities are found to be less than $2.0 \text{ cm}^2/\text{volt sec}$, suggesting that conduction involves electrons in the d level of iron.

1. INTRODUCTION

ELECTRICAL conductivity, Hall effect, and Seebeck effect have been measured on polycrystalline samples of $\alpha\text{Fe}_2\text{O}_3$ containing small deviations from stoichiometry and small amounts of added titanium. These measurements were made in the course of an investigation of the conduction mechanism in oxides whose cations have a partially filled d level. A qualitative discussion of this mechanism was first given by deBoer and Verwey.¹ The addition of titanium to produce an increase in the conductivity of $\alpha\text{Fe}_2\text{O}_3$ has been reported by Verwey and others.² Barth and Posnjak³ show that titanium enters the $\alpha\text{Fe}_2\text{O}_3$ lattice substitutionally as Ti^{4+} , thus producing an Fe^{2+} and maintaining the average charge per cation at three. Verwey points out that the Fe^{2+} acts as a donor center with respect to the surrounding Fe^{3+} ions and that an electron thermally excited from the Fe^{2+} can wander in an environment of Fe^{3+} ions and, under the influence of an external field, produce an electric current. No quantitative theory has been developed to describe such a mechanism. Consequently, the experimental results presented in this paper are interpreted, to a limited extent, in terms of the band picture.

1.1 Preparation of Samples

The Fe_2O_3 used was C. K. Williams Company pigment grade R2899. Titanium was introduced in the form

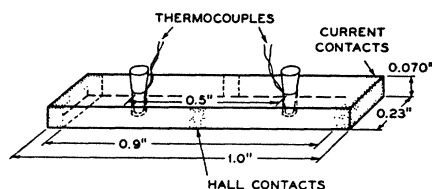


FIG. 1. Diagram of sample showing approximate dimensions and location of contacts and thermocouples.

¹ J. H. deBoer and E. J. W. Verwey, Proc. Phys. Soc. (London) 49, (extra part) (1937).

² E. J. W. Verwey *et al.*, Chemisch Weekblad 44, 705-708 (1948).

³ T. F. W. Barth and E. Posnjak, Z. Krist. 88, 265, 271 (1934).

of TiO_2 obtained as Titanium Pigment Corporation pigment grade Titanox AMO. The oxides were compacted into sample bars using a wax binder obtained in a water emulsion as Socony Vacuum Oil Company Ceremul C. Chemical analyses of these materials are given in the Appendix.

Oxides were mixed in a colloid mill with distilled water slightly acidified with acetic acid. The emulsion was added to the mixture (0.2 cc emulsion per gram of oxide), the wax precipitating from emulsion onto the oxide particles as the acid neutralized the emulsifying agent. Oxides with binder were filtered and dried. Rectangular samples were compacted in a die using a pressure of about one ton per square inch. Two thermocouple holes were drilled through the sample using a No. 60 drill. Samples were heated at 300°C to evaporate the binder and then sintered, under controlled conditions of heating and cooling, at 1100°C for 16 hours. Contacts were painted on the samples using gold or platinum paste containing a small amount of powdered glass (to bond contact metal to oxide) and fired in air at 700°C for 3 minutes. A typical sample is sketched in Fig. 1.

Samples were made of $\alpha\text{Fe}_2\text{O}_3$ and $\alpha\text{Fe}_2\text{O}_3$ containing 0.05, 0.2, and 1.0 atomic percent titanium. One set of samples was sintered in pure oxygen at atmospheric

TABLE I. Composition of samples.

Sample	Atomic % added Ti	Density g/cm^3	Atoms/ cm^3 of Fe	Atoms/ cm^3 of Ti	
1	0.00	5.179	3.977×10^{22}	0.0	Sintered in oxygen
2	0.05	—	3.975×10^{22}	2×10^{19}	
3	0.20	—	3.969×10^{22}	8×10^{19}	
4	1.00	—	3.937×10^{22}	4×10^{20}	
—	—	5.190	4.000×10^{22}	—	
A	0.00	5.211	4.023×10^{22}	0.0	Sintered in $74\text{N}_2 + 2\text{O}_2$
B	0.05	—	4.021×10^{22}	2×10^{19}	
C	0.20	—	4.015×10^{22}	8×10^{19}	
D	1.00	—	3.983×10^{22}	4×10^{20}	

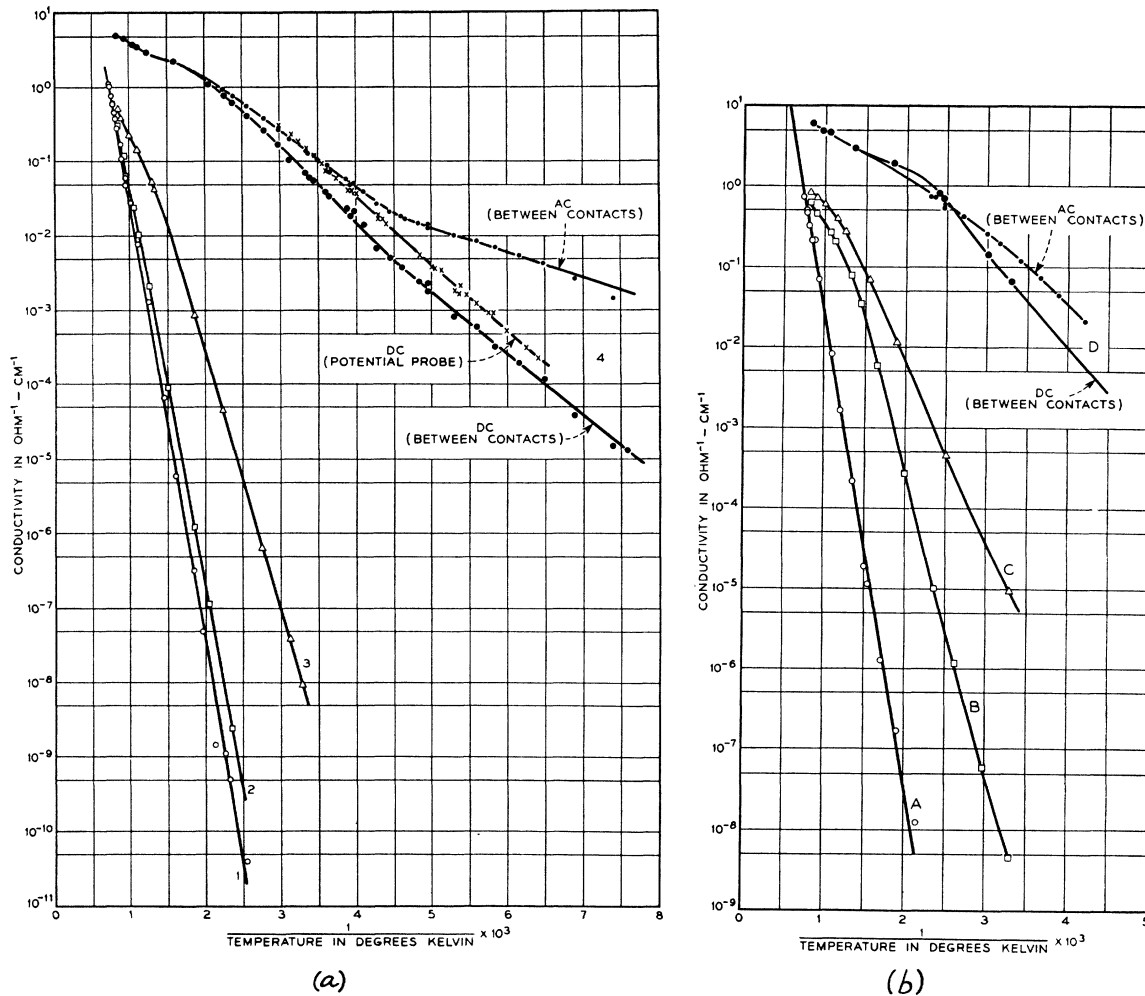


FIG. 2. Conductivity as a function of reciprocal temperature for samples sintered (a) in oxygen; and (b) in $74\text{N}_2 + 2\text{O}_2$. Compositions are given in Table I.

pressure to produce a small metal deficiency in the oxide. A second set of samples was sintered in a slightly reducing atmosphere of $74\text{N}_2 + 2\text{O}_2$ by volume at atmospheric pressure to produce a small metal excess in the oxide. An idea of the departure from stoichiometry of the $\alpha\text{Fe}_2\text{O}_3$ was obtained from a determination of the density of the finely powdered material by displacement in carbon tetrachloride. The density of a sample of $\alpha\text{Fe}_2\text{O}_3$ sintered in air was taken to represent that of a stoichiometric sample since its composition is $\text{Fe}_{2.0005}\text{O}_3$,⁴ a stoichiometric departure too small to detect by the density method used. Assuming a perfect oxygen lattice, the oxidized sample was found to contain an Fe deficit of 2.3×10^{20} atoms per cc and the reduced sample a metal excess of 2.3×10^{20} atoms per cc. Compositions of the samples prepared are shown in Table I. Lattice constants for the samples were determined by K. H.

⁴ J. C. Hostetter and H. S. Roberts, J. Am. Ceram. Soc. 4, 932 (1921).

Storks of these Laboratories. The values found agreed with those given in Wyckoff⁵ for $\alpha\text{Fe}_2\text{O}_3$.

2. EXPERIMENTAL PROCEDURE

The data obtained were resistance, Hall voltage, and Seebeck voltage per degree, all as functions of temperature. Direct current resistance was measured by the potential probe method on low resistance samples where contact resistance was appreciable, and was measured directly between contacts with an ohmmeter on high resistance samples. The field used to produce the transverse Hall voltage was measured with a rotating coil and voltmeter calibrated against a permanent magnet whose field strength had been measured by the Bureau of Standards.

Temperatures above room temperature were measured with platinum, platinum-rhodium thermocouples

⁵ R. W. G. Wyckoff, "The structure of crystals," A.C.S. Monograph No. 19 (Chemical Catalogue Company, New York, 1931), p. 254.

and below room temperature with Chromel *P*, Alumel couples. The couples were wedged with small ceramic cones into the thermocouple holes of the sample as shown in Fig. 1. Seebeck voltage and potential probe voltage were measured between the platinum or alumel leads of the couples. The temperature difference used to produce the Seebeck effect was about 5°C at low temperatures and 25°C at high temperatures. The ambient temperature was taken to be the average of the temperatures measured by the two couples. All dc voltages were measured with a Leeds and Northrup type *K* potentiometer. Current through the sample was measured with a Model 322 Weston milliamperemeter.

After the dc measurements had been made it was realized that grain boundary resistance might be significant in the low resistance samples. To disclose grain boundary resistance, the parallel components of resistance and capacitance were measured as a function of frequency on sample 4 at room temperature using an ac bridge. The ac resistance was found to be the same as the dc resistance up to 10^4 cycles but had decreased to one-third the dc resistance at 10^6 cycles. Because at this point the resistance-frequency curve appeared to have leveled off, 10^6 cycles was used for measuring ac resistance as a function of temperature on samples 4 and *D*. The resistance of the other samples was beyond the limit of the apparatus.

A check of the dc resistance of samples 4 and *D* after all the above described measurements had been made showed that sample 4 had not changed while sample *D*

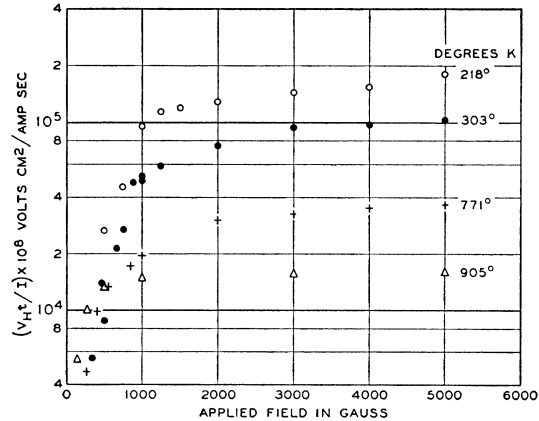


FIG. 3. Dependency of Hall effect on applied field for sample 4.

had increased in dc resistance by a factor of 5. For this reason, more detailed measurements were not made on sample *D* as they were on sample 4. Because of its interesting behavior, measurements of ac and dc resistance, Hall voltage, and Seebeck voltage per degree were made to as low temperatures as possible on sample 4. Similar low temperature measurements were not possible on the other samples because of their high resistance.

3. EXPERIMENTAL RESULTS

Conductivity as a function of reciprocal temperature is shown in Fig. 2(a) for oxidized samples and Fig. 2(b)

TABLE II. Hall effect as a function of temperature with and without applied field.

Sample No.	°K	ΔV_H for $H = \pm 5000$ millivolts	ΔV_H for $H = 0$ millivolts	t cm	I milliamps	$\Delta V_H t^2 \times 10^8 / 2I$ for $H = \pm 5000$	$\Delta V_H t^2 \times 10^8 / 2I$ for $H = 0$
1	583	13.0	9.8	0.190	0.022	5.6×10^9	4.2×10^9
	639	12.2	10.1		0.114	1.03×10^9	8.4×10^8
	701	10.8	8.6		0.70	1.47×10^8	1.17×10^8
	823	1.39	0.94		1.80	7.3×10^6	5.0×10^6
	941	0.36	0.24		10.0	3.4×10^5	2.3×10^5
	967	<0.01			19.6	$<5 \times 10^3$	
2	561	35.7	29.4	0.185	0.0300	1.10×10^{10}	9.1×10^9
	563	38.5	30.2		0.0325	1.09×10^{10}	8.6×10^9
	715	41.6	31.5		3.6	1.07×10^8	8.1×10^7
	835	9.96	5.27		11.0	8.4×10^6	4.4×10^6
	945	1.27	0.88		13.4	8.8×10^5	6.1×10^5
	953	<0.01			13.55	$<7 \times 10^3$	
3	415	42.9	35.9	0.170	0.112	3.26×10^9	2.73×10^9
	546	44.7	35.7		6.5	5.83×10^7	4.66×10^7
	723	5.0	3.7		13.6	3.14×10^6	2.32×10^6
	857	1.48	0.99		14.0	9.0×10^5	6.0×10^5
	933	0.77	0.51		20.0	3.27×10^5	2.16×10^5
	967	<0.005			20.0	$<2 \times 10^3$	
4	222	0.43	0.25	0.147	18.5	1.71×10^5	1.00×10^5
	264	0.50	0.34		19.5	1.81×10^5	1.27×10^5
	307	0.425	0.316		20.0	1.56×10^5	1.16×10^5
	391	0.298	0.227		20.0	1.095×10^5	8.35×10^4
	578	0.162	0.119		20.0	5.95×10^4	4.37×10^4
	737	0.107	0.080		20.0	3.94×10^4	2.94×10^4
	855	0.072	0.048		20.0	2.65×10^4	1.77×10^4
	941	0.023	0.015		20.0	8.45×10^3	5.51×10^3
	951	<0.001			20.0	$<3.7 \times 10^2$	

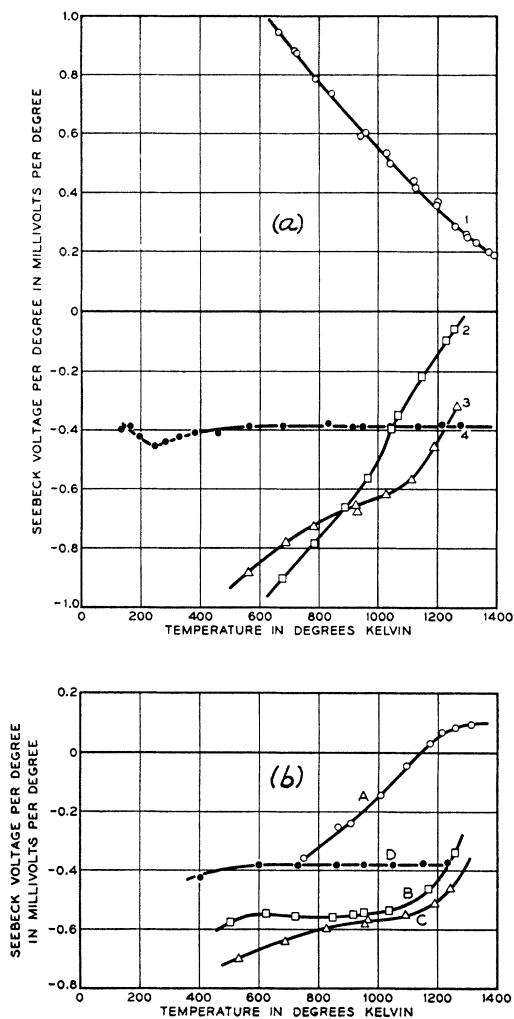


FIG. 4. Seebeck voltage per degree as a function of temperature for samples sintered (a) in oxygen; and (b) in $74\text{N}_2+2\text{O}_2$. Compositions are given in Table I.

for reduced samples. The general behavior of the data appears similar to that obtained from elemental semiconductors (e.g., silicon and germanium) with added impurities. The straight lines obtained for samples 1 and A suggest some type of intrinsic conductivity which also becomes significant in the impure samples at high temperatures. The conductivity plots for samples 1 and A are identical. This would not be expected if holes and electrons from impurity centers produced by oxidation and reduction contribute to conductivity in the usual way. At low temperature the conductivity of impure samples depends upon added impurity. Samples B and C show greater conductivity than samples 2 and 3, respectively. This probably means that impurity centers produced by oxidation cancel some of those produced by titanium. Sample D is nearly the same as sample 4, indicating that the number of effective impurity centers produced by oxidation is small compared with the number from one percent added titanium.

Conductivity results for sample 4 indicate the presence of a small amount of contact resistance which causes a difference between dc conductivity measured between contacts and by potential probe. The presence of grain boundaries having a higher resistance and higher temperature coefficient of resistance than the grains themselves is suggested by comparison of potential probe with ac conductivity for sample 4. The ac conductivity is used in subsequent computations.

Conduction in samples 1 and A may depend upon a mobility mechanism or an excitation mechanism. If excitation of the usual type, theory indicates that conductivity σ in the intrinsic region should vary as

$$\sigma = A \exp \epsilon_0 / 2kT, \quad (1)$$

where A is a constant in $\text{ohm}^{-1} \text{cm}^{-1}$, ϵ_0 is the width of the unallowed band in electron volts, k is the Boltzmann constant in electron volts per degree, and T the absolute temperature in degrees Kelvin. From the conductivity of samples 1 and A, $\epsilon_0 = 2.34 \text{ eV}$ and $A = 2.1 \times 10^4 \text{ ohm}^{-1} \text{cm}^{-1}$.

The Hall coefficient was first measured as a function of

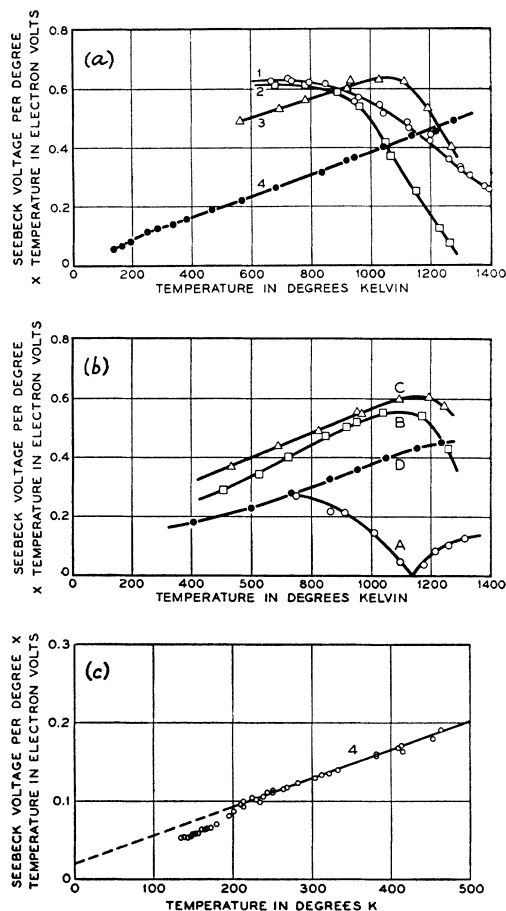


FIG. 5. Seebeck voltage per degree multiplied by temperature plotted as a function of temperature (a) for samples sintered in oxygen; (b) for samples sintered in $74\text{N}_2+2\text{O}_2$; and (c) detailed plot for sample 4. Compositions are given in Table I.

applied field. It was found to depend on applied field in such a way as to suggest that magnetization of the sample was taking place and producing a large enhancement of the field within the sample. This was unexpected since the magnetic susceptibility per gram for these materials is only about 130×10^{-6} .⁶ Results are shown in Fig. 3 for sample 4. Since the effective magnetic field is unknown, the product $R_H H_{\text{eff}} = (V_H t / I) \times 10^8$ has been plotted against applied field for various temperatures. R_H = Hall coefficient in $\text{cm}^2/\text{coulomb}$, H_{eff} = effective magnetic field in gauss, V_H = transverse Hall voltage in volts, t = sample thickness in cm, and I = sample current in amperes. Results in Fig. 3 suggested that saturation magnetization occurred at about $H = 1000$ since, above this value $(V_H t / I) \times 10^8$ increases slowly and linearly with applied field, and that the linear part of the curve resulted from the true Hall effect of the sample. It seemed reasonable to expect, therefore, that R_H for the nonmagnetic part of the sample might be obtained by measuring V_H in the sequence $H = +5000$, $H = 0$, $H = -5000$, $H = 0$ and computing R_H after subtracting the contribution of the magnetization to the Hall voltage as measured when $H = 0$. Results of such measurements for samples 1, 2, 3, and 4 are shown in Table II. The disappearance of Hall voltage above the ferromagnetic Curie point (950°K) indicates that the true R_H for the material cannot be determined from the data in the way described. Carrier concentration computed from Seebeck data predicts a value for V_H just above the Curie point about one decade greater than the limit of the measuring apparatus, consequently, the normal Hall voltage should have been measurable. This apparently small Hall effect may be due to the existence of a mesh-like network of conducting paths in the polycrystalline sample or to peculiarities of the mechanism of d level conduction. The sign of the Hall voltage measured was negative for all samples except for oxidized $\alpha\text{Fe}_2\text{O}_3$ (sample 1) for which it was plus.

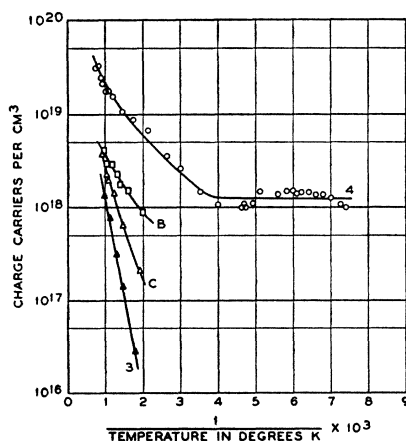


FIG. 6. Charge carrier concentration in the impurity range as a function of reciprocal temperature computed from Seebeck data for samples 3, 4, B, and C.

⁶ F. J. Morin, Phys. Rev. **78**, 819-820 (1950).

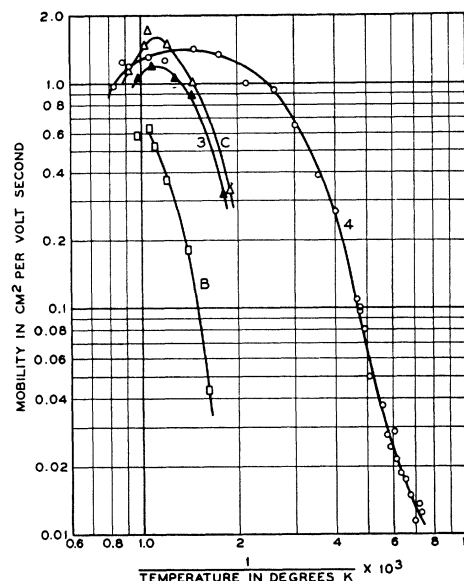


FIG. 7. Electron mobility in the impurity range as a function of reciprocal temperature for samples 3, 4, B, and C.

No further use is made of the Hall data in this paper. However, it is intended to investigate the magnetization effect in more detail, particularly on single crystals, and report on it in a later paper.

The Seebeck voltage per degree as a function of temperature is shown in Fig. 4(a) for oxidized samples and Fig. 4(b) for reduced samples. These data are in agreement with Hall data as to sign. In addition, the Seebeck voltage per degree of reduced $\alpha\text{Fe}_2\text{O}_3$ (sample A) becomes positive above 1140°K . It is not clear why the mechanism which produces the difference in sign of Hall and Seebeck effects for samples 1 and A fails to change their conductivity.

4. FERMI LEVEL, CHARGE CARRIER CONCENTRATION, AND MOBILITY

In this section, Fermi level, charge carrier concentration and mobility are computed in so far as possible using present theory. Charge carrier concentration is within the range where the electron gas may be considered nondegenerate. The symbols and equations to be used in analyzing the data are as follows.

Symbols: e = charge on electron = 1.6×10^{-19} coulomb. m_e = rest mass of electron = 9.11×10^{-28} gram. k = Boltzman constant = 1.38×10^{-16} erg/degree. h = Planck constant = 6.62×10^{-27} erg second. T = absolute temperature in degrees Kelvin. n_e = concentration of conduction electrons = No./ cm^3 . μ = electron mobility in $\text{cm}^2/\text{volt sec}$. σ = conductivity in $\text{ohm}^{-1} \text{cm}^{-1}$. Q = Seebeck voltage per degree in millivolts/degree. ϵ_0 = distance from top of filled band to bottom of conduction band in electron volts. ϵ_F = location of Fermi level from top of filled band in electron volts.

Equations:

Impurity range for electrons

$$\sigma = n_e e \mu_e \quad (2)$$

$$-QT \times 10^{-3} = \epsilon_0 - \epsilon_F + 2.5 \times 10^{-7} kT/e \quad (3)$$

$$n_e = 2(2\pi m_e kT)^{3/2} / h^3 \exp[-(\epsilon_0 - \epsilon_F)e/kT]. \quad (4)$$

Equation (3), the relation between thermoelectric power Q and Fermi level ϵ_F , can be derived as follows. Q is the measure of the entropy flux per unit current due to a temperature gradient.⁷ The current carriers are electrons.

Entropy per electron in the conduction band

$$= (\epsilon_0 - \epsilon_F)e/T + (5/2)k.$$

Entropy flux in field E = electron flux \times entropy/electron

$$= E\mu_e n_e [(\epsilon_0 - \epsilon_F)e/T + (5/2)k].$$

Current density in field E = $E\mu_e n_e e$.

Therefore the entropy flux per unit current

$$= (\epsilon_0 - \epsilon_F)/T + 5k/2e.$$

4.1 Location of the Fermi Level

Observed values of Q have been multiplied by the absolute temperature of observation and QT plotted as a function of absolute temperature in Fig. 5(a) for oxidized samples and Fig. 5(b) for reduced samples. In Fig. 5(c) a detailed plot of QT is shown for sample 4 at low temperatures. These plots necessarily give an incomplete picture of Fermi level behavior since, to determine the Fermi level accurately, the carrier concentration and mobility for both holes and electrons must be known. In the impurity region $-QT$ indicates the distance of the Fermi level below the conduction band, since the impurity centers are donors. As temperature increases and more donors become ionized the Fermi level moves away from the conduction band toward the center of the unallowed band and $-QT$ becomes larger. This behavior is shown for samples 3, 4, *B*, *C*, and *D*. The extrapolation of the impurity region to zero temperature for these samples gives an idea of the location ϵ_D of the donor centers. When, at high temperature, carriers of opposite sign from intrinsic type conductivity become appreciable in relative numbers, QT decreases with increasing temperature as shown by samples 1, 2, 3, *A*, *B*, and *C*. It seems significant that QT for these samples either is positive or is rapidly tending toward a positive value at high temperature. This may mean that hole mobility is greater than electron mobility. More

⁷ C. Herring and M. H. Nichols, *Revs. Modern Phys.* **21**, 185 (1949).

probably, however, a correct explanation of these results depends in some other way upon the mechanism which produces the Seebeck effect.

4.2 Computation of n_e and μ_e

Carrier concentration in the impurity range has been computed from Seebeck data using Eqs. (3) and (4) and is shown as a function of reciprocal temperature in Fig. 6 for samples 3, 4, *B*, and *C*. Electron mobility has been computed from conductivity and carrier concentration using Eq. (2) and is shown in Fig. 7 for samples 3, 4, *B*, and *C*. Results for sample 4 suggest that two mechanisms may be operating, one at low temperatures where conduction changes due to the change in mobility with temperature and a second at higher temperatures where conduction change is more the result of the increase in the number of carriers than the change in mobility. The very low values found for mobility suggest that the conduction is due to electrons confined to the *d* level. In Fig. 6, the intercept of carrier concentration at $1/T=0$ for the various samples suggests that each added titanium donates an order of one electron to the conduction process.

The author is indebted to P. W. Anderson for suggesting that the Hall voltage was caused by magnetization, to J. Bardeen for stimulating discussions of the data, and to C. Herring for Eq. (3).

APPENDIX I

Chemical analysis of materials Fe₂O₃ by quantitative analysis

Fe ₂ O ₃	99.00 percent
SiO ₂	0.06
Fe ²⁺	0.07
Mn	0.08
Al ₂ O ₃	0.04
MgO	0.05
CaO	0.07
Cu	0.0003

TiO₂ by quantitative analysis

TiO ₂	98.1 percent
SiO ₂	0.46
Fe ₂ O ₃	0.01
P ₂ O ₅	0.21
SO ₃	0.06

Ceremul C wax emulsion by spectrochemical qualitative analysis

Na	<0.01 percent
Ca, Fe, Mg, Si	<0.005
Al, Cu, Sn	<0.0005
B, Cr, Ge, Mn, Ni, Pb, Ti	<0.0001

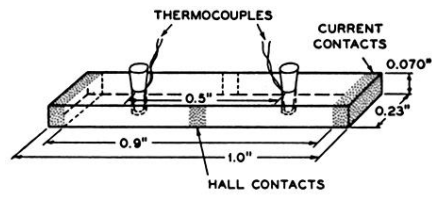


FIG. 1. Diagram of sample showing approximate dimensions and location of contracts and thermocouples.